

# Efficient storage and mobile use of biogas as liquid biomethane

Korbinian Nachtmann, Sebastian Baum, Máté Fuchsz, Oliver Falk, Josef Hofmann

A new treatment concept is intended to make biogas plants more flexible and energy-efficient and to show new marketing possibilities. This is made possible by an innovative low-temperature liquefaction unit, which separates the carbon dioxide portion as dry ice and liquefies the energetic methane at normal pressure. In the laboratory scale, the principle has been successfully implemented and optimised: An adapted multi-stage gas purification, which also works in the absence of oxygen, completely eliminates the fraction of hydrogen sulphide and other contaminants by means of iron preparations and activated carbon filters. By means of clever process control and material selection in the multi-stage heat exchanger system, the carbon dioxide can be separated as snow, thus establishing a continuous process. The resulting dry ice can be sold both energetically and materially as a by-product of gas treatment. In the final liquefaction step, in addition to an energy density of approximately 6.44 kWh per litre of liquid biomethane (based on the calorific value  $H_s$ ), methane purities of up to 99.9% vol. can be achieved depending on the application case.

## Keywords

Cryogenic separation, dry ice, gas purification, biomethane

At the peak of the German biogas boom between 2004 and 2012, the high remuneration for electricity feed-in was attractive, which was guaranteed for twenty years by the Renewable Energy Sources Act (EEG). Thus, for example, locations for biogas plants were selected where there were no consumers for the heat that was generated by power generation. These plants could also be operated economically with pure electricity production. As a result, agricultural biogas plants were created that do not adequately exploit the energetic potential of the biomass being processed. In addition to the lack of energy efficiency, these plants also have an insufficient level of flexibility with respect to power supply by demand, since these plants were designed for full load operation (basic load provision). A load-changing operation with a positive (power increase) or negative (power reduction) control energy, now known as a double superstructure, was not yet planned at the time. The possibilities of storing biogas are limited due to the low energy density at normal pressure. It is, however, desirable to turn biogas into electricity if the demand for electricity is high or if solar and wind energy are not available (compensation of volatile energy producers). The option of cleaning biogas, feeding it into the gas network and thus being able to store it flexibly for a long time only existed for large plants. For smaller plants with gas flows of less than 250 m<sup>3</sup> per hour, as are typical in southern Germany, preparation was too expensive (ADLER et al. 2014).

In the meantime, there are new and innovative ideas on how to implement treatment for small amounts of gas as well as to help improve the energy efficiency of small agricultural facilities in this way (FÖRDERGESELLSCHAFT FÜR NACHHALTIGE BIOGAS- UND BIOENERGIENUTZUNG 2015). A promising approach is

to be presented here: The principle is based on the separation of impurities as well as a pressure-free cryogenic liquefaction unit, which converts the crude gas from the biogas plant into liquefied biomethane (LBM) and industrially replaceable dry ice (solid carbon dioxide). The liquid biomethane is a versatile, easily transportable energy carrier that can be stored for a long time, because of the greatly reduced volume (the storage volume is reduced by a factor of approximately 1,000 compared to biogas). Due to the high energy density of liquid biomethane ( $H_s = 6.44$  kWh per litre compared to approximately 0.0064 kWh per litre of biogas), transport to an energy-efficient power plant is just as feasible as using fuel for lorries (BAUER et al. 2013). In the US, LBM trucks have already become established. Food transports could simultaneously use the low temperatures of the LBM to cool their cargo. The dry ice produced as a „by-product“ is a valuable additional product of the cryogenic process, which can be marketed in various industries at good prices (KOLBINGER 2016).

### **The concept of the processing plant**

The concept of pressure-free cryogenic biogas treatment presented here is based on a specially adapted, upstream gas purification and subsequent low-temperature treatment, which first deposits the carbon dioxide portion of the gas in the form of dry ice and then liquefies the remaining methane (Figure 1). There are two important tasks for gas purification: on the one hand, components that impair the technical functionality and the energy efficiency of the cryoprocess are to be removed. On the other hand, impurities are to be prevented in the carbon dioxide separated as dry ice, which make its marketing more difficult.

During the gas separation, the focus is on stable and constantly operating heat exchangers. On the one hand, trouble-free, long-term operation is to be achieved, i.e. the freezing of the heat exchangers is prevented. For this reason, the freezing carbon dioxide must take the form of snow and not ice. On the other hand, energy-efficient circuit systems must keep the energy input small. The laboratory system designed for this application is an in-house production of the Landshut University of Applied Sciences.

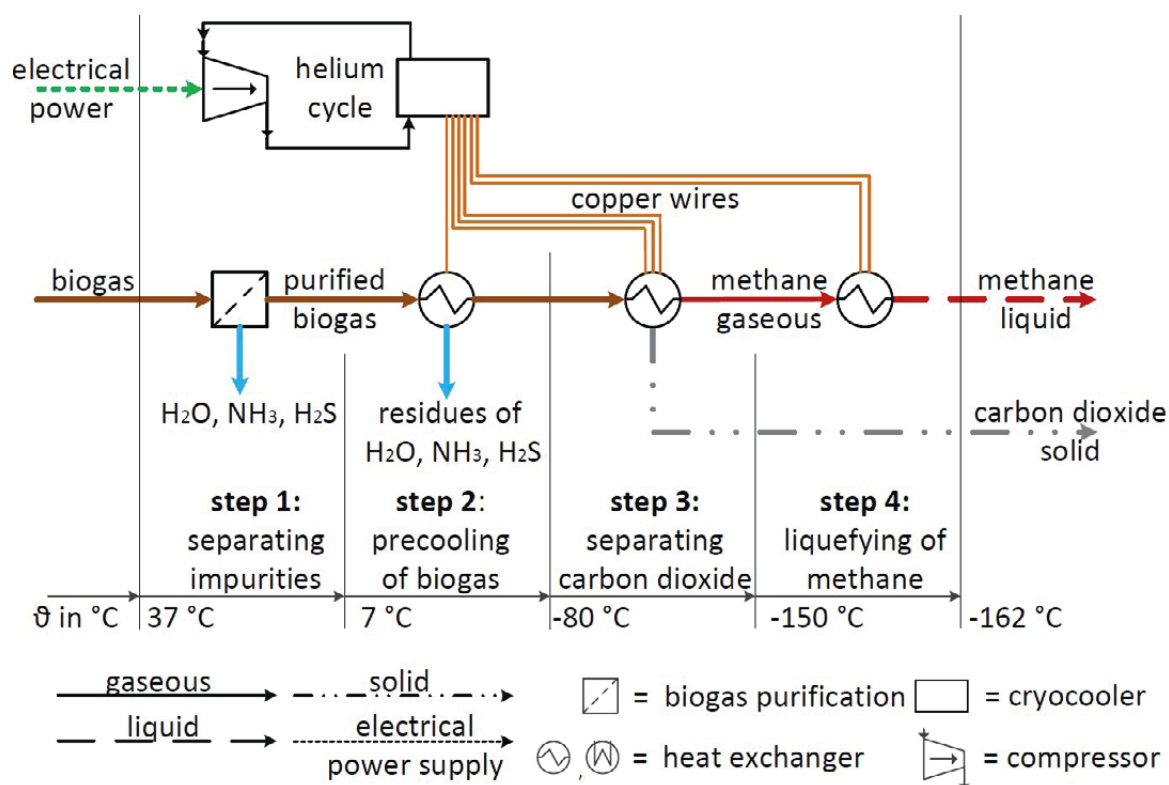


Figure 1: Schematic representation of gas purification and cryogenic gas separation.

In addition to the main components of methane and carbon dioxide, of which (dry) biogas is normally more than 99%, small amounts are mainly hydrogen, ammonia and hydrogen sulphide. Further possible minor components in biogas have already been investigated in other studies: in a large-scale study (DIETRICH et al. 2012), all silanes and siloxanes were below the detection limit for agricultural biogas plants. They were determined by means of gas chromatography-mass spectrometry coupling. Very low concentrations of propane, butane, toluene and other combustible gases could be detected analytically (URBAN et al. 2008). In the case of sulphur compounds, small amounts of two mercaptans were detected (DIETRICH et al. 2012). An analysis of the relevance of all possible trace gases for the overall process showed that only hydrogen sulphide and ammonia have to be regarded as problematic, because they have vapour pressure curves that are nearly identical to those of the carbon dioxide to be separated. The consequence of this is that even the smallest impurities of these toxic and odour-intensive gas components would greatly devalue the dry ice. Both components must therefore be completely removed. For ammonia, its good solubility in water (907 g NH<sub>3</sub> per litre of water at 0 °C) offers the cost-effective separation via a water scrubbing. On the other hand, the toxic hydrogen sulphide can only be separated completely with great effort: The most cost-effective method of biological coarse desulphurisation applied in most biogas plants is unsuitable for the overall process, since gas diluted with oxygen and nitrogen consumes more cooling energy. The absence of oxygen in the biogas creates a special challenge for activated carbon adsorption, because a minimum concentration of 1.5 times the stoichiometric oxygen amount or 0.1–0.5% vol. is required for the functionality and efficiency of the hydrogen sulphide bond to the activated carbon (ARNOLD 2009). If too little oxygen is

present during the contact time, the activated carbon can be irreparably damaged (DONAU CARBON GMBH 2011) or significantly lower  $H_2S$  amounts bound (SITTHIKHANKAEW et al. 2014). Consequently, the gas purification tests focus on an efficient, safe and cost-effective separation of hydrogen sulphide.

In this context, it is important to place a high value on the technology of gas analysis. A complete removal of  $H_2S$  means that this removal must also be continuously documented and ensured. The exact analysis of hydrogen sulphide proportions mainly involves two problems. The first of these is the cross-sensitivity of many sensors to certain gas components (e.g. hydrogen sulphide and hydrogen). The second is the detection limit of trace gases, which for some components, such as hydrogen sulphide, cannot be pushed into the sensory range of the human nose, even with significant technical intervention (POWERS 2004). For this reason, it is productive to implement several analytical methods in parallel and to validate them mutually.

### Cryogenic biogas treatment

The feasibility of low-temperature processes for the treatment of biogas has been discussed for many years. These processes differ in process temperature and pressure. For example, at a pressure of approximately 4 MPa and a temperature of  $-20\text{ }^\circ\text{C}$  (Figure 2), in addition to gaseous methane, liquid  $CO_2$  is also obtained a second product of biogas processing. If, however, the already mentioned advantages of liquid biomethane are to be utilized, then the temperature must be lowered further until methane reaches the boiling curve (approximately  $-88\text{ }^\circ\text{C}$ ). This inevitably leads to the crossing of the solid-vapour area, thus forming solid carbon dioxide in the rectification columns, which in turn leads to problems during processing (AGSTEN 1992).

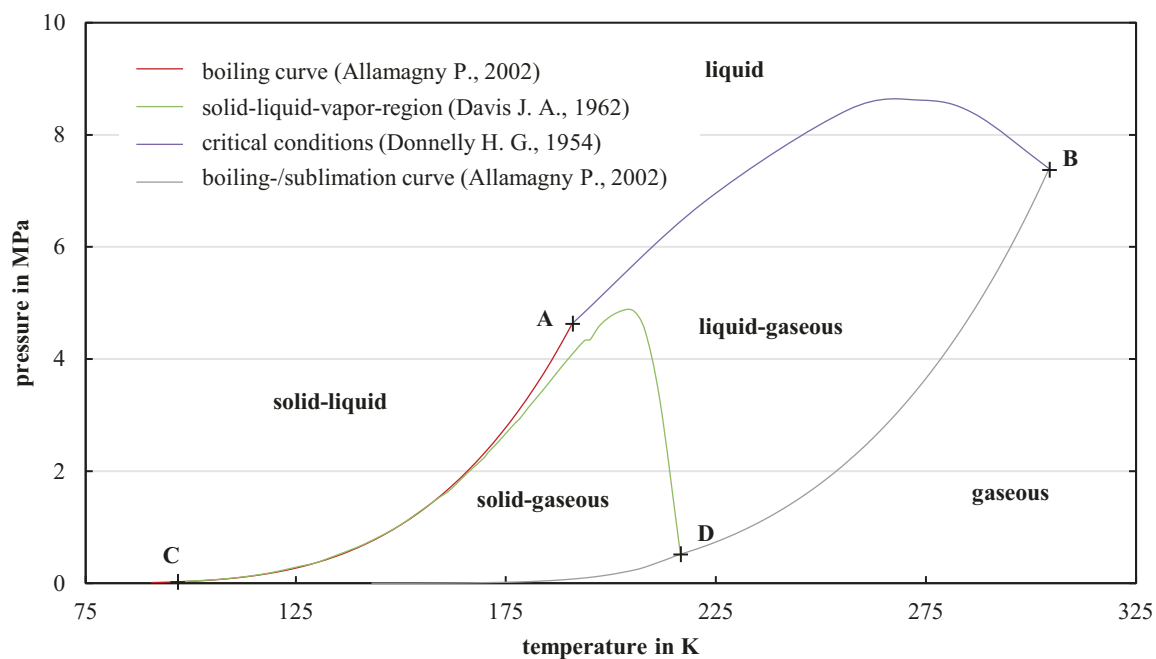


Figure 2: Schematic phase diagram for the carbon dioxide methane system. Changed according to DONNELLY (1954) DAVIS (1962), AGRAWAL and LAVERMAN (1975), ALLAMAGNY (2002). A = critical point  $CH_4$ ; B = critical point  $CO_2$ ; C = triple point  $CH_4$ ; D = triple point  $CO_2$

**Rectification processes** work specifically in the liquid-vapour phase area. Due to the sliding partial pressure, the phase transformation can also take place only at sliding temperatures. Solid carbon dioxide is only expected at a temperature of  $-56^{\circ}\text{C}$  and is avoided as much as possible. The regular defrosting of the columns can also help. By adding alkanes such as propane or butane, the separation capacity of methane and other acidic gases was also increased (JONSSON 2011). From a volume flow of approximately  $50\text{ m}^3$  biogas per hour, this type of biogas cleaning seems to be technically manageable and above all economically viable, despite a high technical effort (SEIME 1997).

**Freezing processes** operate in the solid-vapour phase area. The sublimation lines of the gas mixture have to be considered more precisely for the purity of the methane content. The sublimation lines of carbon dioxide rise greatly from a pressure of approximately 0.5 MPa (Figure 3). A pressure increase has little or no improvement on the purity. The preparation of a gas mixture for a  $\text{CO}_2$  residual gas concentration of 0.5% vol. is an example. Either a temperature of  $-108^{\circ}\text{C}$  and a pressure of 1.5 MPa or a pressure of 0.15 MPa and a temperature of  $-123^{\circ}\text{C}$  is required for this purpose. The liquefaction of the methane amount obtained after the separation is useful in a cryogenic treatment process at  $-161.5^{\circ}\text{C}$  and a pressure of 0.1 MPa.

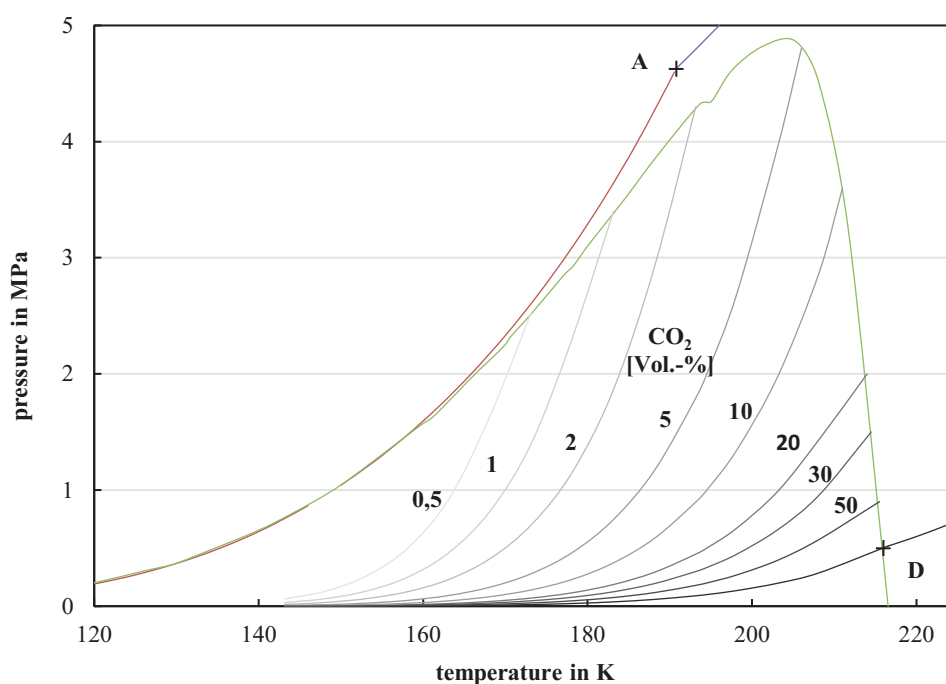


Figure 3: Sublimation lines in the solid-vapour area of  $\text{CO}_2\text{-CH}_4$  mixture in vol. %. Recalculated and modified via the steam pressure curve of  $\text{CO}_2$  according to DONNELLY (1954), DAVIS (1962), AGRAWAL and LAVERMAN (1975), ALLAMAGNY (2002)

The possibility of providing cooling during the freezing process is advantageous to the rectification process. In this case, an external refrigeration circuit can be used, which is not nearly as susceptible to faults as an internal refrigeration circuit. External cooling circuits also have higher overall efficiency levels. Another advantage is that freezing processes have a lower energy requirement for the treatment of biogas into liquid methane compared to rectification processes (AGSTEN 1992).

### State of the art technology

Currently, in addition to the companies Wärttilä (JAKOBSEN 2016), Acrion Technologies (ACRION TECHNOLOGIES 2013, 2015) and Biofrigas (LARSSON 2013), other specialised companies are extracting carbon dioxide and methane as products of biogas processing with their processing plants. The most frequently used procedures and their different concepts, functions and implementation strategies are shown below.

The company GtS (Gastreatment Services bv) from the Netherlands offers complete solutions for biogas processing into compressed biomethane or even liquid biomethane. In the „GPP system“, liquid CO<sub>2</sub> is gained as a by-product through the combined liquefaction and freezing. The cascade cooling system operates with different pressure and temperature levels up to approximately 2.6 MPa and -95 °C (KRAMER 2011). The company Pentair Haffmans, on the other hand, uses two-stage pressure membrane bodies to separate the CO<sub>2</sub> components. Downstream is the cryogenic processing into liquid CO<sub>2</sub>, which makes it possible to produce food quality CO<sub>2</sub> in combination with an activated carbon filter. Plants are in operation in the Netherlands, the UK and Germany (HEIJER 2014, PENTAIR HAFFMANS 2015). The company Prometheus Energy is currently optimising a process of LNG production (liquefied natural gas) for biogas processing. One plant that has been operating commercially since 2006 produces liquid biomethane, which is mainly produced from landfill gas. A fleet of more than 2,000 buses in Orange County (California) is thus supplied with LBM from landfill gas. Carbon dioxide is frozen for processing. The cooling capacity is provided by liquid nitrogen (GREEN CAR CONGRESS 2007, BARCLAY 2015). The company Cryo Pur applied for the first patent for the separation of CO<sub>2</sub> from biogas already in January 2001. The production of liquid CO<sub>2</sub> (Purity 99.9% vol.) and liquid methane (99.4% vol.) is achieved using a three-stage process. The specified power requirement of 0.5 kWh<sub>e</sub>/m<sup>3</sup> Biogas for separation and liquefaction is classified as low (CRYO PUR 2016).

These commercially available processes extract liquid carbon dioxide and gaseous or liquid methane as biogas processing products by working at high pressure and low temperatures. The process described here does not require a compaction of the biogas so as to obtain liquid methane and solid carbon dioxide as processing products.

### The State of Science and Research

In the last few years, individual research institutes, such as the Technical University of Dresden or the University of Eindhoven, have repeatedly dealt with projects for the development of cryogenic biogas processing on a laboratory scale. The continued development of the experimental setups for industrial applicability tested on a small scale is slow or has not advanced at all. In addition to the research results of HAGEN (2001), JONSSON (2011) and TUINIER et al. (2010), the following developments are of particular interest:

HULLU et al. (2008) have developed a multi-stage low-temperature separation process for biogas with colleagues at the Eindhoven University of Technology in the Netherlands. The process, operating

at a maximum pressure of 4 MPa and the lowest temperature of  $-90^{\circ}\text{C}$ , provided methane as a product that is ready for liquefaction. In the next development steps, the rectification process is mainly concerned with increasing the methane concentration and lowering the methane slip. Due to the high compressor capacity, the developments are currently concentrated on a module with a flow rate of  $2,250\text{ m}^3/\text{h}$ . REICHL et al. (2015) developed a system for low-temperature biogas processing. After pre-purification with activated carbon filters, the biogas is fed to the two-stage pressure unit. This is followed by compression to 0.8 MPa followed by expansion to 0.5 MPa. The second compressor stage compresses the biogas to the process pressure of approximately 2.0 MPa. The subsequent cascade cooling allows for a temperature of approximately  $-50^{\circ}\text{C}$ , which is not yet low enough for biogas processing. Currently, the reactor is being converted to a minimum process temperature of  $-100^{\circ}\text{C}$ . By using low-cost components and extracting liquid carbon dioxide as a by-product in addition to gaseous biomethane, there is great potential in this research project. Chun-Feng Song from the University of Tsukuba (Japan) has been researching the freezing behaviour of carbon dioxide from flue gases since about 2011. An SC-1 Stirling refrigeration machine from Stirling-Cryogenics takes care of the refrigeration. The cleaning performance was investigated in detail as a function of the parameters of cooling temperature and volume flow. The maximum recovery rate was 96% vol. of the carbon dioxide contained in the flue gas of a coal-fired power plant. However, the energy balance for flue gases cannot be transferred to biogas. In order to better understand the process of hoar frost generation, numerical calculations followed in 2013. The direct influence of the heat transfer from the steadily growing ice layer was demonstrated both experimentally and numerically. Targeted energy analyses completed the existing experimental programme in 2014 (SONG et al. 2012, SONG et al. 2013, SONG et al. 2014).

### The Freezing Process

For the processing of biogas, it is recommended to use heat exchangers optimised for each sub-process (SEIME 1997). The sub-processes (Figure 1) are as follows:

- Heat exchanger 1: Pre-cooling the biogas to the sublimation temperature of  $\text{CO}_2$ , precipitation of impurities such as water or ammonia
- Heat exchanger 2: Desublimation of the  $\text{CO}_2$  contained in the biogas
- Heat exchanger 3: liquefaction of the  $\text{CH}_4$  contained in the biogas

The pre-cooling of the biogas to  $-80^{\circ}\text{C}$  follows first. Here, it is possible to condense or freeze any residual concentrations of trace gases and water. The resulting binary gas mixture of carbon dioxide and methane is then cooled to approximately  $-150^{\circ}\text{C}$  to fully freeze the gaseous  $\text{CO}_2$  and thereby to obtain dry ice. In the last step, the residual gas is cooled to below  $-162^{\circ}\text{C}$  and the condensation of the gaseous methane amount into liquid biomethane occurs. Possible amounts of nitrogen or oxygen would be removed from the reactor at this point in gaseous form.

Figure 4 shows the vapour pressure curve of carbon dioxide in detail (VDI 2013), which was expanded by the extrapolation of the known values by equation 1. Depending on the desired purity of the methane to be obtained, different results are possible by varying the process parameters. If a  $\text{CO}_2$  residual gas concentration of less than 50 ppm should be reached in the methane gas and the methane should be liquefied near atmospheric pressure, the biogas must be cooled to approximately  $-158^{\circ}\text{C}$ . If a  $\text{CO}_2$ -residual concentration of 1,000 ppm  $\text{CO}_2$  is sufficient, the cooling of the gas flow to approximately  $-136^{\circ}\text{C}$  is sufficient. In thermodynamics, this effect is known as fractional sublima-

tion as a function of gas pressure (KUPRIANOFF 1953). The theoretical behaviour of the gases derived from diagrams and tables should be practically confirmed by tests in the further course of this thesis.

$$\text{Vapour pressure } p_{TX} = 7367,82186 \cdot e^{-[0,00074 \cdot (T-246,16809)^2]} \quad (\text{Eq. 1})$$

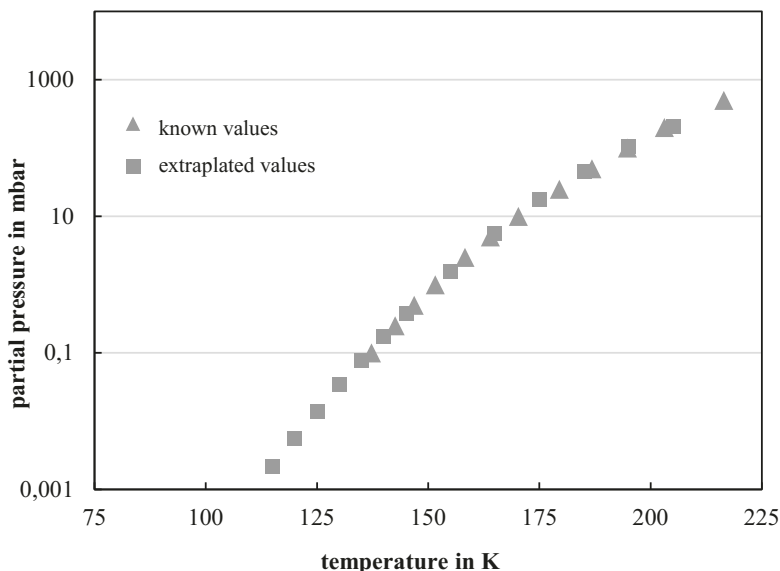


Figure 4: Vapour pressure curve of carbon dioxide with values extrapolated by „e-square function“

### Snow or ice

The icing over of the heat exchanger stands in the way of the continuous long-term operation of the processing plant. It can be prevented by working in the liquid-vapour range, but with the disadvantages that were just described. On the other hand, the alternative of regularly defrosting the heat exchangers does not seem to make sense from an energy and economic point of view. However, the freezing can also be prevented if the carbon dioxide solidifies as snow instead of ice. The density of the resulting dry ice is the decisive parameter here (TITOV 1976). Thus a low dry ice density leads to loosely adherent snow layers, while a high dry ice density can be blamed for the icing over of the heat exchangers (RUDENKO 1986). In addition to the effects of the physical properties of the heat exchangers, such as surface energy density and roughness on the snow or ice formation, the influences of the process parameters, such as volume flow, flow velocity, sliding temperature difference, gas composition, etc., are also to be investigated and demonstrated.

### Materials and Methods

On the basis of the specifications of the low temperature unit, a laboratory biogas plant with a 250 litre fermenter fill capacity has been built that can be used to produce a daily gas volume of about 200 litres. In addition, a significantly smaller double fermenter with a filling volume of 2 x 30 litres was used, which allowed a parallel operating mode and thus a direct comparison of treatment versions. The systems were fed with a substrate mixture of corn silage and molasses in order to achieve a continuous gas production and in particular high concentrations of the trace gas hydrogen sulphide.

The studies on gas purification consisted of experiments on coarse desulphurisation, in which iron preparations (Ferrosorp DG) were placed directly in one of the two 30-litre fermenters, as well as a series of tests for the purification of the produced gas by means of adsorption columns and gas-washing bottles. The gas flow of raw and pure gas was measured with a drum gas meter. In the 30-minute interval, automated quantification of the gas components took place using a gas analysis system from Awite Bioenergie GmbH (Awi-Flex Series 7). The biogas was first cooled by means of a circulating cooler (water saturation) and the gas humidification was subsequently reduced to the desired level (75–80%) by means of a heat bath in order to maintain a constant moisture level in the containers filled with activated carbon, even in the case of fluctuating outside temperatures. Finally, the reaction gas flow was brought to 5 °C with a sample gas cooler, the corresponding amount of water was condensed and experiments with drying agents were carried out. Measurement and data logging was carried out via an Almemo system (Ahlborn) (Figure 5).



Figure 5: Test equipment for gas cleaning (section) with adsorption columns in the water bath (left), sample gas cooler (rear right) and drying columns (rear left) (© Hochschule Weihenstephan)

A total of 13 different active carbon preparations from seven manufacturers (Cabot Norit Activated Carbon, CarboTech GmbH, Carbon Service & Consulting GmbH & Co. KG, Chemviron Carbon, Desotec, Danube Carbon GmbH, Jacobi Carbons GmbH) as well as two iron-based adsorbents were tested. The activated carbon consisted of partly untreated, partly impregnated and partly doped products, which are particularly suitable for use in the biogas sector. Silica gel (Roth, Ø 2–5 mm) and zeolite (Roth, 3Å, Ø 1.6–2.5 mm) were used for the drying experiments. In addition to measurements with the Awite system's electrochemical sensors (0–20 ppm for clean gas, 0–2,000 ppm for crude gas), additional measurements were taken via Dräger gas tubes (for ammonia, hydrogen sulphide and mercaptans) as well as measurements via gas chromatography and were then compared with each other.

The tests on the absorption capacity of hydrogen sulphide by activated carbon or other adsorptive filling materials were determined according to the US ASTM standard D6646-03 (ASTM INTERNATIONAL 2015), on which most manufacturers of activated carbon products also base their specifications. However, the specifications of the standard were not implemented, which contradicted the background of the research project. Thus, the raw biogas produced was used and not the H<sub>2</sub>S/N<sub>2</sub> mixture prescribed in the standard with sulphur contents of 10,000 ppm. In addition, an air mixture was done away with for the above reasons.

### Cryogenic temperature tests

In order to be able to permanently maintain the low temperatures of –162 °C necessary for processing and to minimize heat losses, the construction of a cryogenic test reactor (Figure 6) was practical, the structure of which is explained below.

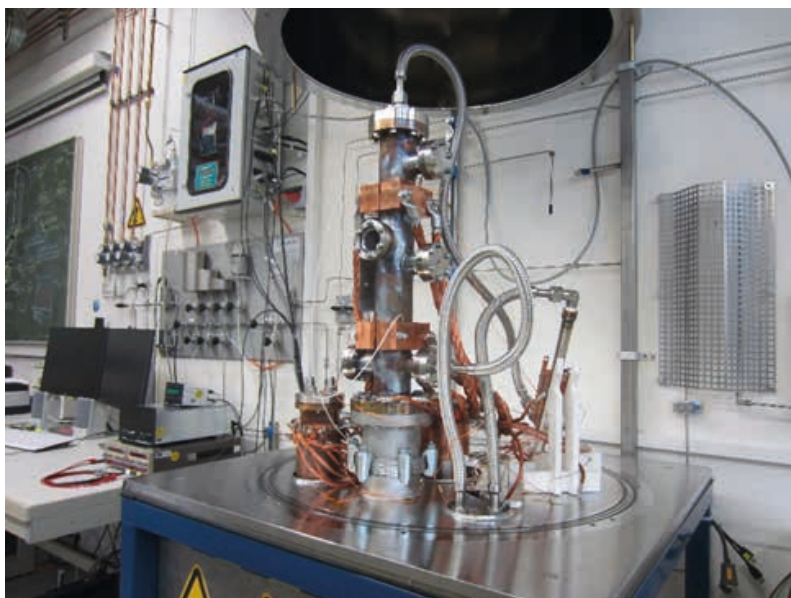


Figure 6: Heat exchanger under the high vacuum bell (© HAW Landshut)

A Gifford-McMahon cold head was used for the cold supply of the laboratory. At temperatures of up to  $-240^{\circ}\text{C}$ , this can provide a cooling capacity of approximately 200 watts. The cooling of the required helium compressor ( $8 \text{ kW}_{\text{el}}$ ) was supplied by a water-air cooler ( $6 \text{ kW}_{\text{el}}$ ). The heat losses must be reduced as much as possible for a continuous operation of the heat exchangers. Heat losses due to convection can almost be completely excluded by working in the high vacuum range. Heat losses from radiation are to be largely reduced by means of electropolished surfaces and the use of a multi-layer thermofoil (multiple reflection/thermal shield). Heat conduction losses can be almost completely avoided by using suitable materials such as PTFE, PEEK or a very thin-walled construction of the heat exchangers.

Thanks to the combination of pulse width modulation and PID control units, the control system, which was built using the software program LABView, allowed a constant temperature maintenance of  $\pm 1^{\circ}\text{C}$  for all three heat exchangers. For the cooling of the heat exchangers, the heat was deflected to the cold head via copper strands (Figure 6). The tubular heat exchanger made of corrosion-free steel 1.4404 (A4L) was held at a constant temperature level of approximately  $-150^{\circ}\text{C}$  in order to almost fully separate the  $\text{CO}_2$  content as dry ice through low-temperature desublimation. The gas mixture of  $\text{CO}_2$  and  $\text{CH}_4$  already pre-cooled to  $-80^{\circ}\text{C}$  was introduced into the tube from the upper end and crystallised on the inside of the heat exchanger coated with PTFE (Safecoat 571 from the company Impreglon) as solid  $\text{CO}_2$ . The remaining residual gas, which mainly consisted of methane, was removed at the end of the tubular heat exchanger laterally to the downstream heat exchanger for liquefaction. Furthermore, a vacuum-tight sight glass was installed in the centre of the tubular heat exchanger in order to visually detect and document the formation of  $\text{CO}_2$  crystals. The high-vacuum reactor is also designed for all experiments up to a range of  $p = 1 \times 10^{-7}$  mbar and  $t = -240^{\circ}\text{C}$  and is suitable due to the use of standardised ISO-K and ISO-CF flanges.

The freezing unit is designed for a maximum gas volume flow of 60 liters of biogas per hour, but is expandable to a flow rate of up to 300 l/h. By means of mass flow valves, synthetic gas of pure  $\text{CH}_4$  and pure  $\text{CO}_2$  can be mixed in any concentration ratios. For measuring data acquisition (pressure, temperature, volumetric flow, gas composition, etc.) and plant control or regulation, a valve cluster and a National Instruments Compact Rio unit were used. The most important sensors used for the determination of the gas purity and for the proof of a functional preparation are listed in Table 1.

Table 1: Measuring instruments used for concentration determination

| Measuring instruments  | Field of application   | Measurement range  | Accuracy <sup>1)</sup>                     | Special feature   |
|--|--|--|--|---|
| SWG100biogas<br>NDIR sensors<br>(MRU Messgeräte für<br>Rauchgase und Um-<br>weltschutz GmbH) | Gas composition at the<br>inlet of the cryogenic<br>system (gas from the<br>fermenter)                     | CO <sub>2</sub> 0–100 %<br>CH <sub>4</sub> 0–100 %<br>O <sub>2</sub> 0–10 %<br>H <sub>2</sub> 0–100 %    | ± 1,2 %<br>± 1,8 %<br>± 0,2 %<br>± 2,0 %   | Electrochemical sensors for<br>the measurement of oxygen<br>and hydrogen  |
| SWG100biogas<br>NDIR sensors<br>(MRU Messgeräte für<br>Rauchgase und Um-<br>weltschutz GmbH) | Gas composition at the<br>outlet of the cryogenic<br>system (pure methane<br>and pure carbon diox-<br>ide) | CO <sub>2</sub> 0–100 %<br>CH <sub>4</sub> 0–100 %<br>CO <sub>2</sub> 0–0,5 %<br>CH <sub>4</sub> 0–0,5 % | ± 1,0 %<br>± 1,0 %<br>± 40 ppm<br>± 40 ppm | Daily calibration with:<br>100 % CH <sub>4</sub> ; 100 % CO <sub>2</sub> ;<br>100 % N <sub>2</sub> ; 1000 ppm/<br>1000 ppm CH <sub>4</sub> /CO <sub>2</sub> re-<br>quired the start of experi-<br>ment to ensure accuracy |
| digital mass flow control-<br>ler (MKS Instruments<br>Germany GmbH)                          | Adjusting the mass flow<br>or volume at the inlet of<br>the reactor  | 0–500 sccm/min<br>0–500 sccm/min   | ± 0,7 %<br>± 0,7 %                         | Volume flow is automatically<br>regulated using the meas-<br>ured values of the SWG<br>100biogas  |
| IR OEM CO <sub>2</sub> -high & low<br>IR OEM CH <sub>4</sub> -high<br>Dynament Limited       | Review of the function-<br>ality capability of the<br>SWG100biogas   | CO <sub>2</sub> 0–100 %<br>CH <sub>4</sub> 0–100 %<br>CO <sub>2</sub> 0–5 %                              | ± 2,0 %<br>± 2,0 %<br>± 0,1 %              | Analysing the gas volume<br>flow at the inlet/outlet of<br>the cryogenic system alter-<br>nating  |

<sup>1)</sup> Relative to the maximum measuring range.

An experiment was carried out as follows for example: At the start, the two vacuum pumps and the cold head unit were put into operation. The vacuum bell and the entire pipeline system were then evacuated. After a cooling time of about three hours, the low-temperature separation tests were started. A Bühler sample gas pump pumped the biogas that was previously generated in the biogas plant from the gas storage sacks into the first measuring instrument (SWG100biogas, company MRU). After the gas composition was determined, the gas was passed directly to the two digital mass flow valves (the company MKS). The programme created in LABView automatically regulates the volume flow of exactly one litre of biogas per minute as a function of the gas composition. If the CH<sub>4</sub>-CO<sub>2</sub> ratio in the biogas is changed, a mass flow adjustment occurs due to the greatly different gas densities of methane and carbon dioxide.

After determining the inlet pressure and the temperature of the now conditioned biogas, this is passed to the three heat exchangers for gradual cooling. In order to measure the purity of the resulting methane, the composition of the gas was temporarily examined by using the second SWG100 biogas measuring instrument. After a test time of 6 to 8 hours, the mass flow valves and the cold head were switched off and the reactor was purged with pure nitrogen. Subsequently, the frozen carbon dioxide was sublimed and fed back to the second MRU measuring instrument in order to detect methane deposits.

In order to determine the influence of the process parameters on the freezing process, numerous tests with varying gas compositions, flow rates, cooling rates and cooling temperatures were evaluated.

## Results and Discussion

The resulting ammonia amounts fluctuated between 0 and 9 ppm and could be quickly, economically and completely removed from the gas flow by means of the gas-washing bottle. As expected, the re-

removal of the hydrogen sulphide to a constant level of 0 ppm proved to be the more difficult task. The initial values of the  $H_2S$  in the raw gas were subject to greater fluctuations depending on the feed with 600–1,900 ppm. The coarse desulphurisation in the fermenter by means of the iron hydroxide agent Ferrosorp DG to a  $H_2S$  value of about 100 ppm was achieved without problems. The product quantities to be used for this purpose with starting concentrations of approximately 700 ppm are shown in Figure 7. The reduction to the desired 100 ppm level was also successful at higher initial concentrations of about 1,400 ppm.

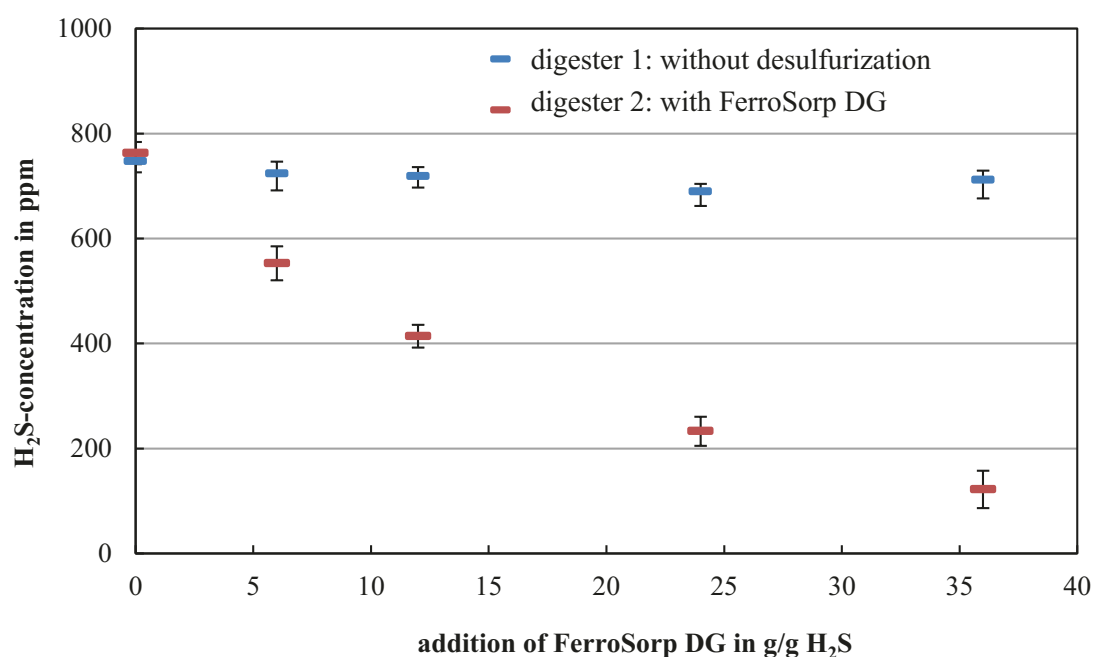


Figure 7: Hydrogen sulphide reduction in the double fermenter. The addition of Ferrosorp in fermenter 2 leads to a reduction to 100 ppm  $H_2S$  while the control (fermenter 1) remains at the level of 700 ppm (average values 8–14 days after conversion of the dosage)

The elaborate tests for fine cleaning showed a wide range of the suitability of the examined activated carbon or the iron-based preparations. Some of the products (activated carbon A, B, H, I ...) were not able in the dominant difficult conditions to lower the  $H_2S$  concentrations to the ASTF standard set goal of <50 ppm, let alone to the 0 ppm required for the cryogenic process. It is known from the literature that the absence of oxygen leads to the fact that current adsorption principles are impaired or not possible at all (SITTHIKHANKAEW et al. 2014). A few products (activated carbon E & M, iron product N) were nevertheless convincing. Table 2 shows the individual measurement results during the pass with high raw gas concentrations of 1,300–1,800 ppm  $H_2S$ . The core parameter of the experiments, the adsorption capacity, which indicates how much hydrogen sulphide per gram of adsorbent can be bound, remains at an unsatisfactorily low level for all products tested against the background of high activated carbon prices.

Table 2: Adsorption capacities of activated carbon and iron products according to the ASTM standard

| Adsorbent          | Fill amount | H <sub>2</sub> S content in raw gas (agent) | Time to breakthrough (>50 ppm) | Raw gas until breakthrough | H <sub>2</sub> S until breakthrough | Adsorption capacity |
|--------------------|-------------|---|--------------------------------|----------------------------|-------------------------------------|---------------------|
|                    | in g        | in ppm                                      | in min                         | in litres                  | in g                                | in g/g              |
| Activated carbon A | 112.36      | 1,515                                       | 0                              | 0                          | 0                                   | 0                   |
| Activated carbon B | 59.83       | 1,413                                       | 0                              | 0                          | 0                                   | 0                   |
| Activated carbon C | 62.71       | 1,431                                       | 1,920                          | 332                        | 0.72                                | 0.012               |
| Activated carbon D | 53.3        | 1,355                                       | 1,530                          | 280                        | 0.58                                | 0.011               |
| Activated carbon E | 71.02       | 1,842                                       | 5,520                          | 1,289                      | 3.61                                | 0.051               |
| Activated carbon F | 64.26       | 1,367                                       | 3,540                          | 558                        | 1.16                                | 0.018               |
| Activated carbon G | 89.13       | 1,596                                       | 1,590                          | 387                        | 0.94                                | 0.011               |
| Activated carbon H | 56.38       | 1,434                                       | 0                              | 0                          | 0                                   | 0                   |
| Activated carbon I | 59.49       | 1,551                                       | 0                              | 0                          | 0                                   | 0                   |
| Activated carbon J | 72.34       | 1,503                                       | 0                              | 0                          | 0                                   | 0                   |
| Activated carbon K | 69.96       | 1,492                                       | 0                              | 0                          | 0                                   | 0                   |
| Activated carbon L | 76.85       | 1,553                                       | 1,500                          | 316                        | 0.75                                | 0.010               |
| Activated carbon M | 79.36       | 1,515                                       | 4,322                          | 915                        | 2.11                                | 0.027               |
| Iron product N     | 69.42       | 1,662                                       | 1,4670                         | 2,513                      | 6.35                                | 0.091               |
| Iron product O     | 51.05       | 1,606                                       | 0                              | 0                          | 0                                   | 0                   |

### Goal reached by product combination

At H<sub>2</sub>S concentrations of about 1,100 ppm, in some products, the hydrogen sulphide contained in them could be removed completely (up to the breakthrough, continuously 0 ppm in the clean gas). None of the examined products for desulphurisation were able to constantly keep the H<sub>2</sub>S concentration at 0 ppm at an even higher load (approximately 1,300–1,800 ppm H<sub>2</sub>S in raw gas) (Figure 8). Rather, the values usually fluctuated in the single-digit range (0–9 ppm), which matches the results of KÖCHERMANN et al. (2015), who were also unable to fully free artificial gas mixtures with activated carbon of H<sub>2</sub>S under oxygen-free conditions. Only lowering the H<sub>2</sub>S values through coarse desulphurisation in the fermenter or adding a coarse filter before the activated carbon fine cleaning was successful and at the same time led to a significant improvement in the adsorption capacity. This is confirmed by previous studies that exhibited an increased absorption capacity and cleaning capacity of the activated carbon at lower initial concentrations of the trace gases (BAGREEV et al. 2005). The iron product N is particularly suitable as a coarse filter for oxygen-free desulphurisation before the activated carbon: it showed a cleaning performance superior to the other products, is cheaper than the high-quality activated carbon and could be regenerated easily by a simple storage in the air. The cleaning performance with the regenerated product differed only slightly from that in the first use.

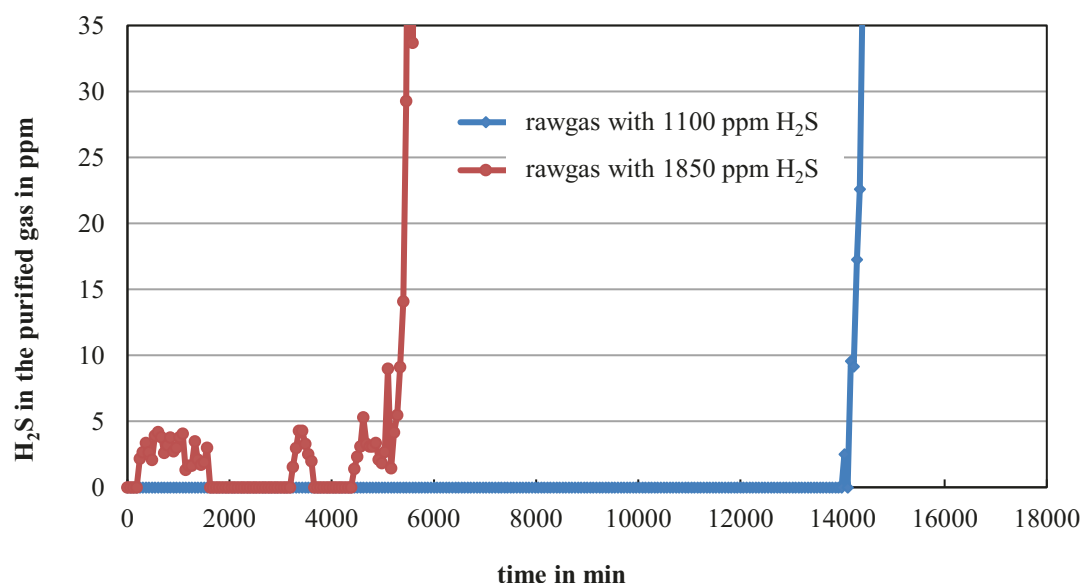


Figure 8: Comparison of the cleaning performance of „activated carbon E“ with different H<sub>2</sub>S output concentrations. While the clean gas at 1,100 ppm H<sub>2</sub>S in the raw gas remains at 0 ppm up to the breakthrough (loading capacity 0.067 g H<sub>2</sub>S/g), the clean gas concentration at 1,850 ppm in the raw gas fluctuates in the low single-digit ppm range (loading capacity 0.051 g H<sub>2</sub>S/g).

Further attempts to optimise the separation of hydrogen sulphide through an appropriate adjustment of the parameters (gas moisture, temperature) led to noticeable specific improvements in the use of individual activated carbon products. Based on these findings, no general recommendations can be made. The partly contradictory results (some products require, for example, a low gas humidity, others a high gas humidity for an optimal yield) are also found in the technical literature (HERDIN et al. 2000, SITTHIKHANKAEW et al. 2014). The gas humidity was reduced to 2 grams of water per standard cubic metre after cleaning with the sampling gas cooler and silica gel. The use of zeolites (molecular sieves) is suitable for separating even more water from the gas flow and achieving degrees of drying that correspond to dew point temperatures below  $-20\text{ }^{\circ}\text{C}$  (ARNOLD 2009). Since this was not necessary for the proper operation of the cryogenic unit, these were not used for economic reasons.

The results show that the desired gas quality of 0 ppm NH<sub>3</sub> and H<sub>2</sub>S can be achieved permanently and cost-effectively even at high concentrations in the raw gas if a coarse desulphurisation in the fermenter is combined with two suitable adsorption units in succession with activated carbon or iron preparations. Neither H<sub>2</sub>S and other sulphur compounds (mercaptans) nor ammonia in measurable amounts ( $< 0.2\text{ ppm}$ ) are then found in the clean gas. The selection of the adsorbents should be made carefully, as there are technically significant differences and, economically, large savings are also possible.

### Product purity of methane and carbon dioxide

Figure 9 graphically shows the purity of  $\text{CH}_4$  after cryogenic treatment. The  $\text{CO}_2$  residual concentration according to Figure 10 is on average less than 3,500 ppm or 0.35% vol. for the test duration shown. The methane purity is 99.65% or more. The outliers of the measurement curves can be explained by declining and subsequently subliming carbon dioxide crystals. Further tests show that even with lower flow rates, even higher purities can be achieved, since the residence time and thus also the cooling time increases with the decrease of the volume flow. If the process is carried out too close to the liquefaction point of methane, small amounts of liquid methane are also separated in the freezing heat exchanger. The purity of the resulting dry ice is correspondingly reduced. However, a faster flow through the reactor leads to higher  $\text{CO}_2$  concentrations in the purified product gas, since the gas can no longer be cooled sufficiently to the predetermined temperatures.

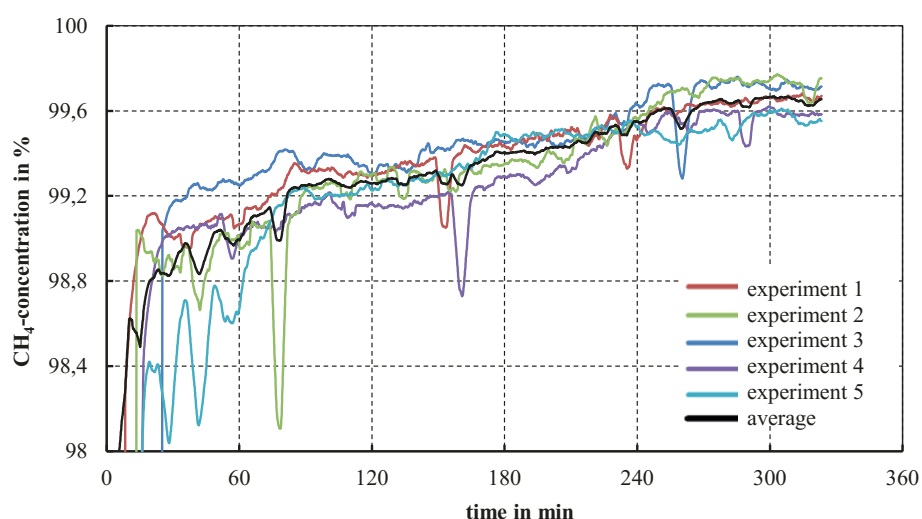


Figure 9: Methane content of the product gas after cryogenic treatment. An excerpt of a measurement series with synthetic biogas is shown (55 %  $\text{CH}_4$  and 45 %  $\text{CO}_2$ )

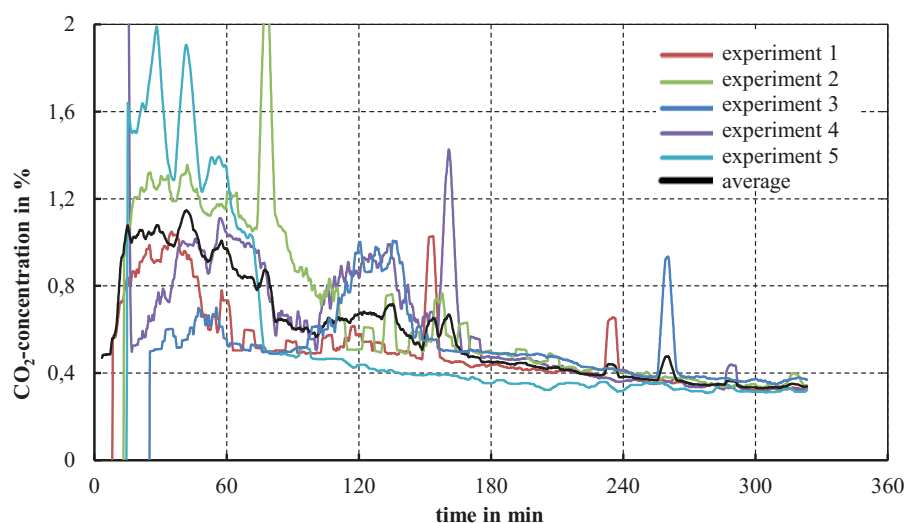


Figure 10: Carbon dioxide content of the product gas after cryogenic treatment. An excerpt of a measurement series with synthetic biogas is shown (55 %  $\text{CH}_4$  and 45 %  $\text{CO}_2$ ).

At the end of the test, the experimental reactor was repeatedly evacuated and purged with nitrogen. After switching off the cold head unit, the frozen carbon dioxide sublimated slowly and was tested for purity in the gaseous state the next day. In addition to an average carbon dioxide content of 98.5% vol., an average methane content of 98 ppm was specified. The remaining 1.5% vol. are attributable to the nitrogen of the multiple purging processes as well as diffusion losses of the gas storage bags. The very low methane content served as the determining factor for quality in any case. To ensure a higher purity of the CO<sub>2</sub> fraction, it is planned to expand the laboratory with a shut-off valve between the freezer and the condenser.

The crystal formation of the CO<sub>2</sub> remaining in the reactor could be visually detected and evaluated by using the sight glass unit. This evaluation led to the confirmation of the measurement theory (HILZ 1940, HAUSEN 1948), according to which local over-saturation can occur in the event of laminar flow. The consequences are snow formation in the gas flow or loosely adhering CO<sub>2</sub> snow on the inner surface of the heat exchanger tube. The explanation of this phenomenon is provided by the Lewis coefficient, the ratio of the coefficient of thermal conductivity or heat transfer coefficient and diffusion number or mass-transfer coefficient. The following phenomenon appears to be present (ULLMANN 1962):

- Up to the beginning of the precipitation of the carbon dioxide, there is no reason for a different concentration distribution
- If carbon dioxide crystals precipitate on the cooled wall, the carbon dioxide concentration at the site concerned is reduced. Thus there is a concentration gradient between the tube wall and the tube centre
- Carbon dioxide diffuses transversely to the direction of flow towards the wall
- The beginning of the carbon dioxide precipitation leads to a reduction in the carbon dioxide concentration of the entire mixture flow
- Local over-saturation phenomena are thus possible

If the mass transport takes place more quickly than the transport of heat, sub-saturation occurs. In the opposite case, over-saturation occurs (LINDE 1950). Figure 11 visualises this phenomenon over the course of time for an experiment with synthetic biogas (50% vol.CH<sub>4</sub> and 50% vol.CO<sub>2</sub>).

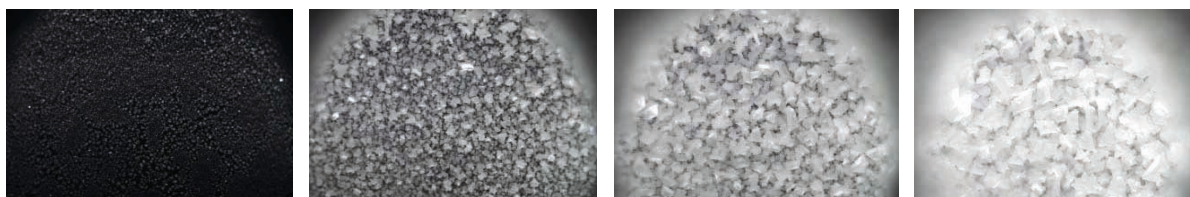


Figure 11: CO<sub>2</sub> crystals on the heat exchanger wall after 1 h, 2 h, 3 h, 4 h of test duration (© HAW Landshut)

In summary, it can be determined that the icing of the heat exchangers can very likely be temporarily avoided by operation in the laminar flow area. The transition from laminar to turbulent tube flow takes place at a Reynolds number of approximately 2,300. Taking into account other factors such as wall roughness, the roughness of the snow layers or the turbulence at the gas inlet of the heat transfer, reductions are still to be made with respect to the Reynolds number to be used. „From the overall considerations, it is advisable to set the speed as low as possible below half the value of the critical value in the case of laminar tests if, despite any snow deposits, you still want to avoid a turbu-

lent flow for a certain amount of time“ (HILZ 1940). Long-term operation of the cryogenic freezing unit (more than 20 h) has been demonstrated. The disadvantage of the low volumetric flow is almost equal to the advantage of the very high purity (RISCHE 1957). The dry ice is to be removed from the bottom of the heat exchanger at regular intervals.

About 0.9 kg of dry ice can be obtained per standard cubic metre of raw biogas with a carbon dioxide content of 45%. The usage possibilities are also varied here: in addition to the cooling of foodstuffs or use in beverage technology, innovative technical applications such as blasting motors or other technical components are also possible. The big advantage of the dry ice blasting method is the residue-free sublimation of the carbon dioxide (SPUR et al. 1999). Above all the following properties of solid carbon dioxide are of particular interest (KUPRIANOFF 1953):

- Very low sublimation temperature of 195 K
- Elimination of the melt water (water ice)
- Large cold supply per unit of volume (2.5 times of water ice)
- Antibacterial effect of CO<sub>2</sub> gas on the refrigerated goods

### Energy efficiency

An example scenario shows a possible application area of the process: during the summer months, it is not possible to use all of the heat produced by biogas (Figure 12, A). Moreover, the yield of regeneratively generated electricity via photovoltaic systems is very high at this time. A previously calculated proportion of the biogas produced in the summer can now be fed to dry ice and liquid biomethane for further processing (Figure 12, B). Thus, the separation of generation and consumption of large amounts of energy is decoupled both as regards time and location. This makes it possible to energise the liquid biomethane while simultaneously fully using the heat and cold in heat-operated, decentralised CHP plants, even if the corresponding demand is given. The resulting dry ice can be used energetically or materially. Due to the high energy density of the liquid methane and the good insulation properties of the transport and storage containers, the losses during transportation and storage are negligible (NACHTMANN 2012). The energetic use of the storage and evaporation losses (boil off gases) is state of the art, for example transport vehicles are simply equipped with a gas engine.

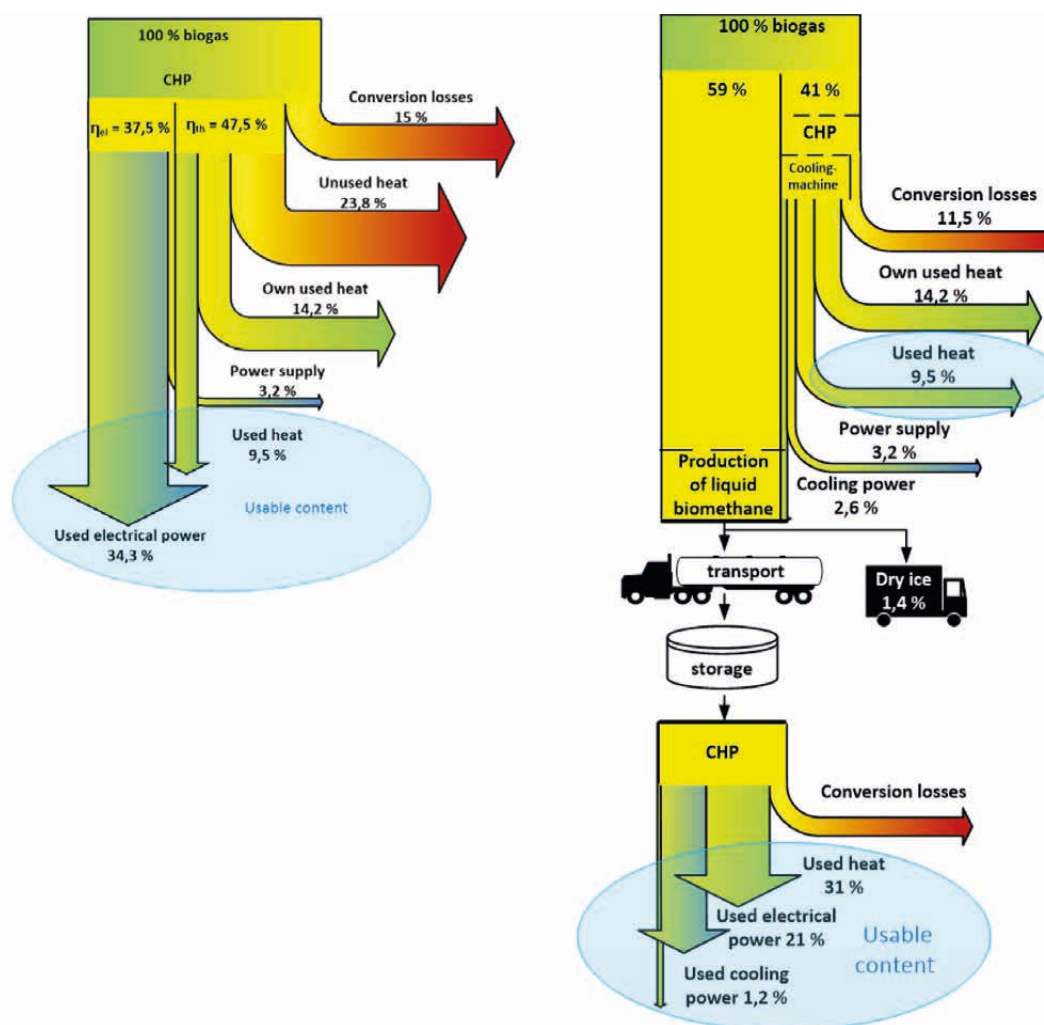


Figure 12: A) Theoretical degree of efficiency of biogas utilisation, state of the art, electricity-operated CHP; B) Theoretical degree of efficiency of biogas utilisation with liquid biomethane production and storage, heat-operated and decoupled for decentralised use in a CHP. The degrees of efficiency of the combined heat and power plant (CHP) as well as the own heat and power demand were assumed as follows: power-operated CHP  $\eta_{el} = 37.5\%$  and  $\eta_{th} = 47.5\%$ ; Heat-operated  $\eta_{el} = 35.0\%$  and  $\eta_{th} = 52.0\%$ ; Own electricity/heating biogas plant demand 9% and 30%. Heat used = heat for heating residential and commercial buildings (depending on plant size)

## Conclusions

In the laboratory scale, it was shown that both the adapted gas purification and the subsequent separation work using a pressureless freezing process. The products, high purity liquid biomethane and dry ice in marketable quality, can be produced continuously. The numerous laboratory tests allowed a technical and economic optimisation of the treatment concept and serve as the basis for a large-scale technical implementation. Due to scale effects, however, a scale-up also leads to adjustments to the technical concept and thus to further research requirements. In many areas it is likely possible to make use of existing technology: for example, it is advisable to produce the required cold via a boil-off cold machine instead of with helium compressor cold-head cooling and thus to significantly increase the efficiency of the plant once again. It seems sensible to implement the concept in a modular manner, i.e. to develop a fixed unit of the processing plant, which is then installed several times in paral-

lel. Such a module with a liquefying capacity of 25 m<sup>3</sup> raw gas per hour corresponds approximately to the electrical power of a biogas CHP of 50 kW<sub>el</sub>. For a typical biogas plant size of 500 kW<sub>el</sub>, 10% of the gas quantities from the electricity generation could be used with a module and liquefied into biomethane. If necessary, however, significantly more modules and a liquefaction of 30, 50 or even 80% could be useful. The utilisation routes (regulation energy supply, fuel use, chemical raw material) are diverse and must be adapted to the infrastructure and the needs of the operators. An intelligent system is ideally created that uses regenerative surplus current from wind or solar energy flexibly for the conversion of biogas into LBM. Parts of it could be used as a fuel for independent supply, while other parts could be used in the event of a power shortage in the CHP. Due to the high energy density of the LBM of 6.44 kWh/l, transport to a modern and efficient gas power plant is also a possible option (BAUER et al. 2013). Only one of the modules described above would produce more than half a tonne of dry ice per day. With skilful marketing, the additional product of dry ice can yield interesting additional revenue of up to 25 cents/kg (JÄGER 2014, KOLBINGER 2016).

Starting in 2020, the 20-year EEG subsidies for the first biogas plants will expire. If the sun and wind-independent operation of the German biogas plants is kept at least at the current level, innovative plant concepts, such as the cryogenic conversion of biogas into liquid biomethane described here, must exist and be used.

A future of biogas plants based on basic load current generation will not exist from the point of view of the authors. This is because construction consortia are already offering PV power for 0.03 USD/kWh and less today (BLOCHE-DAUB et al. 2016). The competitiveness with electric power from other renewable energies, such as wind power or photovoltaics, cannot be achieved on this basis in the medium to long term. Economically viable and energy-efficient concepts, which focus not only on electricity, but also on heat, mobility and the provision of raw materials for the chemical industry, can show biogas plant operators perspectives outside of state subsidy programmes.

## References

- Acron Technologies (2013): Landfill Gas to Liquid Methane with Acron's CO<sub>2</sub> Wash™. <http://www.acron.com/Ingfromlfg.htm>, accessed on am 5 June 2015
- Acron Technologies (2015): Technologies Acron Technologies, Inc: Renewable Fuels and CO<sub>2</sub>. [http://www.midwestchptap.org/Archive/pdfs/090407\\_Ohio/Brown.pdf](http://www.midwestchptap.org/Archive/pdfs/090407_Ohio/Brown.pdf), accessed on 11 June 2015
- Adler, P.; Billig, E.; Brosowski, A.; Daniel-Gromke, J.; Falke, I.; Fischer, E.; Grope, J.; Holzhammer, U. (2014): Leitfaden Biogasaufbereitung und -einspeisung. Hg. Fachagentur Nachwachsende Rohstoffe, Gülzow
- Agrawal, G.M.; Laverman, R.J. (1975): Phase Behavior of the Methane-Carbon Dioxide System in the solid-vapor region. In: *Advances in Cryogenic Engineering*. Ed. Timmerhaus, K.D., Boston, MA/s.l., Springer US, pp. 327–338
- Agsten, R. (1992): Methanverflüssigung aus Biogas – Verfahrenskonzepte und Ökologiepoteziale. *Luft- und Kältetechnik* 4, S. 162–164
- Allamagny, P. (2002): *Encyclopedie des Gaz*. Amsterdam, Elsevier
- Arnold, M. (2009): Reduction and monitoring of biogas trace compounds. VTT Tiedotteita Research Notes 2496, pp. 1–84
- ASTM International (2015): Standard test method for determination of the accelerated hydrogen sulfide breakthrough capacity of granular and pelletized activated carbon, West Conshohocken, PA (USA) (D6646 – 03), D6646 – 03
- Bagreev, A.; Katikaneni, S.; Parab, S.; Badosz, T.J. (2005): Desulfurization of digester gas. Prediction of activated carbon bed performance at low concentrations of hydrogen sulfide. *Catalysis Today* 99(3-4), pp. 329–337, <http://dx.doi.org/10.1016/j.cattod.2004.10.008>

- Barclay, J.A. (2015): Biogas to LNG of Prometheus Energy. Natural Gas Vehicle Technology Forum. [http://www1.eere.energy.gov/cleancities/pdfs/barclay\\_nov08.pdf](http://www1.eere.energy.gov/cleancities/pdfs/barclay_nov08.pdf), accessed on 5 July 2015
- Bauer, F.; Persson, T.; Hulteberg, C.; Tamm, D. (2013): Biogas upgrading - technology overview, comparison and perspectives for the future. *Biofuels, Bioproducts and Biorefining* 7(5), pp. 499–511, <http://dx.doi.org/doi.org/10.1002/bbb.1423>
- Bloche-Daub, K.; Kaltschmitt, M.; Witt, J.; Janczik, S. (2016): Erneuerbare Energien. *Globaler Stand 2015*. BWK Das Energie-Fachmagazin 68(7/8), S. 60–80
- Cryo Pur (2016): Valorize biogas with bio-LNG and bioCO<sub>2</sub>. A more efficient valorization of biogas. <http://www.cryopur.com/en/index.html>, accessed on 8 September 2016
- Davis, J.A. (1962): Solid-liquid-vapor phase behavior of the methane-carbon dioxide system. *AIChE Journal* 8(4), pp. 537-539
- Dietrich, R.-U.; Oelze, J.; Spieker, C.; Spitta, C. (2012): Kombinierte Reformierung von Biogas zur Synthesegas- Erzeugung und Verstromung mittels SOFC-Hochtemperatur-Brennstoffzelle. Gemeinsamer Schlussbericht, [http://www.zbt-duisburg.de/fileadmin/user\\_upload/01-aktuell/05-publikationen/06-Projektberichte/AiF16126N-Abschlussbericht\\_Kombiref.pdf](http://www.zbt-duisburg.de/fileadmin/user_upload/01-aktuell/05-publikationen/06-Projektberichte/AiF16126N-Abschlussbericht_Kombiref.pdf), accessed on 13 March 2014
- Donau Carbon GmbH (2011): Aktivkohle zur Abscheidung von Schwefelwasserstoff, Frankfurt. <http://www.donau-carbon.com/downloads/h2s-abscheidung.aspx>, accessed on 2 June 2015
- Donnelly, H.G. (1954): Phase Equilibria in the Carbon Dioxide-Methane System. *Industrial and Engineering Chemistry* 46(3), pp. 511–517
- Fördergesellschaft für nachhaltige Biogas- und Bioenergienutzung (Hg.) (2015): Progress in Biomethane Mobility. Decentralised production and direct utilisation. Proceedings of the International Conference in Schwäbisch Hall, 27.–28.10.2015, Kirchberg an der Jagst, IBBK
- Green Car Congress (2007): Prometheus Produces World's First Commercial LNG from Landfill Gas; Targeted for Public Transit Fuel. [http://www.greencarcongress.com/2007/01/prometheus\\_prod.html](http://www.greencarcongress.com/2007/01/prometheus_prod.html), accessed on 5 June 2015
- Hagen, M. (2001): Adding gas from biomass to the gas grid, Swedish Gas Center
- Hausen, H. (1948): Einfluß des Lewisschen Koeffizienten auf das Ausfrieren von Dämpfen aus Gas-Dampf-Gemischen. *Angewandte Chemie* 20(7), S. 177–183
- Heijer, N.d. (2014): Haffmans Biogas Upgrading. Turning Biogas Into Biomethane & Green CO<sub>2</sub>. <http://groengas.nl/wp-content/uploads/2012/12/1.3-BIOGAS-UPGRADING-TURNING-BIOGAS-INTO-BIOMETHANE-GREEN-CO2.pdf>, accessed on 25 June 2015
- Herdin, G.; Gruber, F.; Kuffmeier, R.; Brandt, A. (2000): Solutions for siloxane problems in gas engines utilizing landfill and sewage gas. *ICE (American Society of Mechanical Engineers), Alternative Fuels, Dimethyl Ether and Natural Gas Engines* 3, pp. 101–110
- Hilz, R. (1940): Verschiedene Arten des Ausfrierens einer Komponente aus binären, strömenden Gasgemischen. *Zeitschrift für die gesamte Kälte-Industrie* 47, S. 34
- Hullu, J. de; Maassen, J.; van Meel, P.A.; Shazad, S.; Vaessen, J. (2008): Comparing different biogas upgrading techniques. Final report. Quartettkarte, Technische Universiteit Eindhoven
- Jäger, A. (2014): Marktanalyse für die Verwertung von Kohlenstoffdioxid in fester Form. Bachelorarbeit, Hochschule Landshut
- Jakobsen, A. (2016): Wärtsilä liefert richtungsweisende bioHybrid-Anlage nach Deutschland. <http://www.wartsila.com/deu/medien/veroeffentlichung/veroeffentlichung-lokale/20-12-2016-w%C3%A4rtsil%C3%A4-liefert-richtungsweisende-biohybrid-anlage-nach-deutschland>, accessed on 21 March 2017
- Jonsson, S. (2011): Cryogenic biogas upgrading using plate heat exchangers. Sweden, Chalmers University of Technology
- Köchermann, J.; Schneider, J.; Matthischke, S.; Rönsch, S. (2015): Sorptive H<sub>2</sub>S removal by impregnated activated carbons for the production of SNG. *Fuel Processing Technology* 138, pp. 37–41, <http://dx.doi.org/10.1016/j.fuproc.2015.05.004>
- Kolbinger, Q. (2016): Betrachtung des Marktpotenzials eines Verfahrens zur kryogenen Aufbereitung von Biogas. Abschlussarbeit, Hochschule Landshut

- Kramer, S. (2011): Biogas Upgrading. Greenhouse as energy source, Netherlands, <http://www.gastreatmentservices.nl/en/>, accessed on 15 May 2015
- Kuprianoff, J. (Hg.) (1953): Die feste Kohlensäure. Herstellung und Verwendung, Stuttgart, Ferdinand Enke Verlag
- Larsson, M. (2013): Biofrigas AB initiates cooperation with Borås Energy and Environment AB., Gothenburg
- Linde, H. (1950): Über das Ausfrieren von Dämpfen aus Gas-Dampfgemischen bei atmosphärischem Druck. Zeitschrift für angewandte Physik 2, S. 49–59
- Nachtmann, K. (2012): Verflüssigung und Speicherung von Biomethan durch das Tieftemperatur-Desublimationsverfahren. Analyse einer neuen Methode zur Herstellung von Flüssigerdgas aus Biogas. Masterarbeit, Hochschule Ansbach
- Pentair Haffmans (2015): Haffmans Biomethane & Green CO<sub>2</sub>. from Biogas to Biomethane. <http://www.haffmans.nl/resources/images/267.pdf>, accessed on 5 June 2015
- Powers, W. (2004): The Science of Smell Part 1: Odor perception and physiological response., Iowa University, University Extension, Ames, Iowa
- Reichl, J.; Alber, K.; Bai, X.; Mang, H.P.; Li, Z.; Yin, F. (2015): Challenges in the development of a cryogenic biogas upgrading unit with CO<sub>2</sub> recovery. In: Progress in Biomethane Mobility. Decentralised production and direct utilisation, Ed. IBBK Fachgruppe Biogas GmbH, Kirchberg an der Jagst
- Rische, E.A. (1957): Ausfrieren von Dämpfen aus Gas/Dampf-Gemischen bei erzwungener Rohrströmung. Chemie-Ing.-Techn. 29(9), S. 603–615
- Rudenko, N.Z. (1986): Einfluß der Ausfrierbedingungen von Kohlendioxid aus Gasgemischen auf die Dicke und Dichte der sich bildenden Reifschicht. холодильная техника 5, S. 21–26
- Seime, D. (1997): Biogasreinigung bei tiefen Temperaturen. Dissertation, Technische Universität Dresden
- Sitthikhankaew, R.; Chadwick, D.; Assabumrungrat, S.; Laosiripojana, N. (2014): Effects of humidity, O<sub>2</sub>, and CO<sub>2</sub> on H<sub>2</sub>S adsorption onto upgraded and KOH impregnated activated carbons. Fuel Processing Technology 124, pp. 249–257, <http://dx.doi.org/10.1016/j.fuproc.2014.03.010>
- Song, C.; Kitamura, Y.; Li, S. (2014): Energy analysis of the cryogenic CO<sub>2</sub> capture process based on Stirling coolers. Energy 65, pp. 580–589, <http://dx.doi.org/10.1016/j.energy.2013.10.087>
- Song, C.; Kitamura, Y.; Li, S.; Jiang, W. (2013): Analysis of CO<sub>2</sub> frost formation properties in cryogenic capture process. International Journal of Greenhouse Gas Control 13, pp. 26–33, <http://dx.doi.org/10.1016/j.ijggc.2012.12.011>
- Song, C.; Kitamura, Y.; Li, S.; Ogasawara, K. (2012): Design of a cryogenic CO<sub>2</sub> capture system based on Stirling coolers. International Journal of Greenhouse Gas Control 7, pp. 107–114, <http://dx.doi.org/10.1016/j.ijggc.2012.01.004>
- Spur, G.; Uhlmann, E.; Elbing, F. (1999): Dry-ice blasting for cleaning. Process, optimization and application. Wear 233–235, pp. 402–411, [http://dx.doi.org/10.1016/S0043-1648\(99\)00204-5](http://dx.doi.org/10.1016/S0043-1648(99)00204-5)
- Titov, V. (1976): Studie zu Ausfrierprozessen von Kohlendioxid aus Rauchgasen. холодильная техника 10, S. 22–27
- Tuinier, M.J.; Annaland, v.S.; Kramer, G.J.; Kuipers, J.A.M. (2010): Cryogenic carbon dioxide capture using dynamically operated packed beds. Chemical Engineering Science 65(1), pp. 114–119, <http://dx.doi.org/10.1016/j.ces.2009.01.055>
- Ullmann, W. (1962): Beitrag zum Problem der Übersättigung binärer Gasgemische im Bereich tiefer Temperaturen. Dissertation, TU Dresden
- Urban, W.; Girod, K.; Lohmann, H. (2008): Technologien und Kosten der Biogasaufbereitung und Einspeisung in das Erdgasnetz. Ergebnisse der Markterhebung 2007–2008, [http://publica.fraunhofer.de/eprints/urn\\_nbn\\_de\\_0011-n-948875.pdf](http://publica.fraunhofer.de/eprints/urn_nbn_de_0011-n-948875.pdf), accessed on 11 March 2014
- VDI (2013): VDI-Wärmeatlas 2013. Berlin, Heidelberg, Springer-Verlag

## Authors

**Korbinian Nachtmann** and **Prof. Dr. Josef Hofmann** work at Landshut University of Applied Sciences, Am Lurzenhof 1, 84036 Landshut.

**Dr. Sebastian Baum**, **Máté Fuchsz** and **Prof. Dr. Oliver Falk** work at Weihenstephan-Triesdorf University of Applied Sciences in the field of renewable energies technology in the faculty LE (Agriculture and Food Economy), Am Staudengarten 1, 85354 Freising, email: sebastian.baum@hswt.de.

## Acknowledgements

The authors thank the Bavarian State Ministry of Economic Affairs and Media, Energy and Technology for financing the research project.